Chapter – 5

Mechanical Properties of Ultrafine-Grained Low Carbon Steel

5.1 Mechanical Properties of Ultrafine-Grained Low Carbon Steel Produced by ECAP

Figure 5.1 represents engineering stress and plastic engineering strain curves for as-received and ECAPed low carbon steel. The as-received material has the lowest strength (UTS 367 MPa) with maximum total elongation of 41% (Figure 5.1 and Table 5.1).

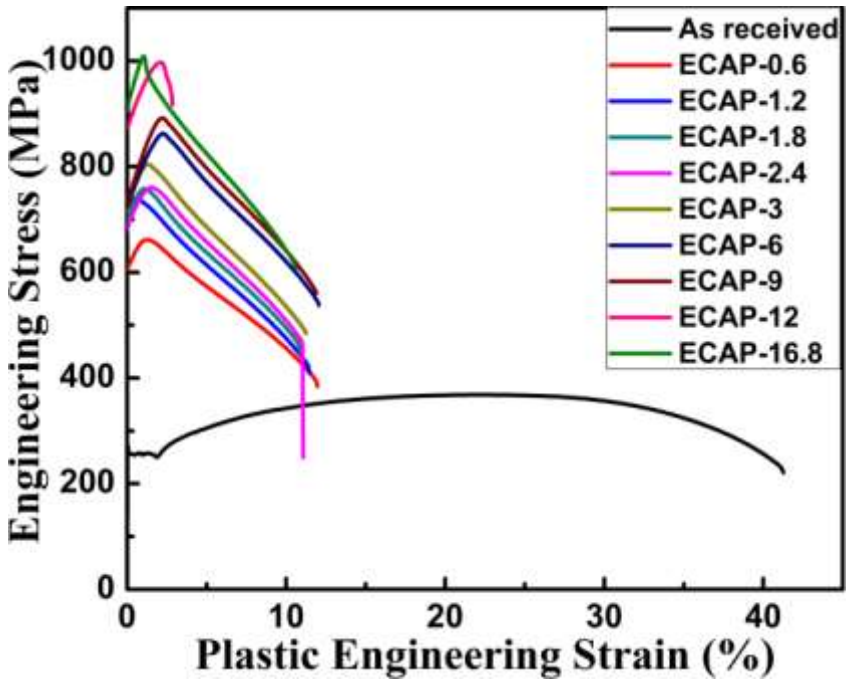

Figure 5.1 Engineering stress and plastic engineering strain curve of low carbon steels.

When the as-received material is ECAPed, strength increases rapidly in the initial passes and gets saturated at higher strain level (Figure 5.2). UTS is highest at ε_{vm} = 16.8 with lowest uniform elongation of 1% (Figure 5.3). These results indicate that the strength increases but ductility is decreased with increase in imposed strain. Hardness increases rapidly in initial passes, but after that its rate of increase is low. After ε_{vm} = 9, no significant improvement in strength is observed upto ε_{vm} = 16.8 (Figure 5.4, Table 5.1).

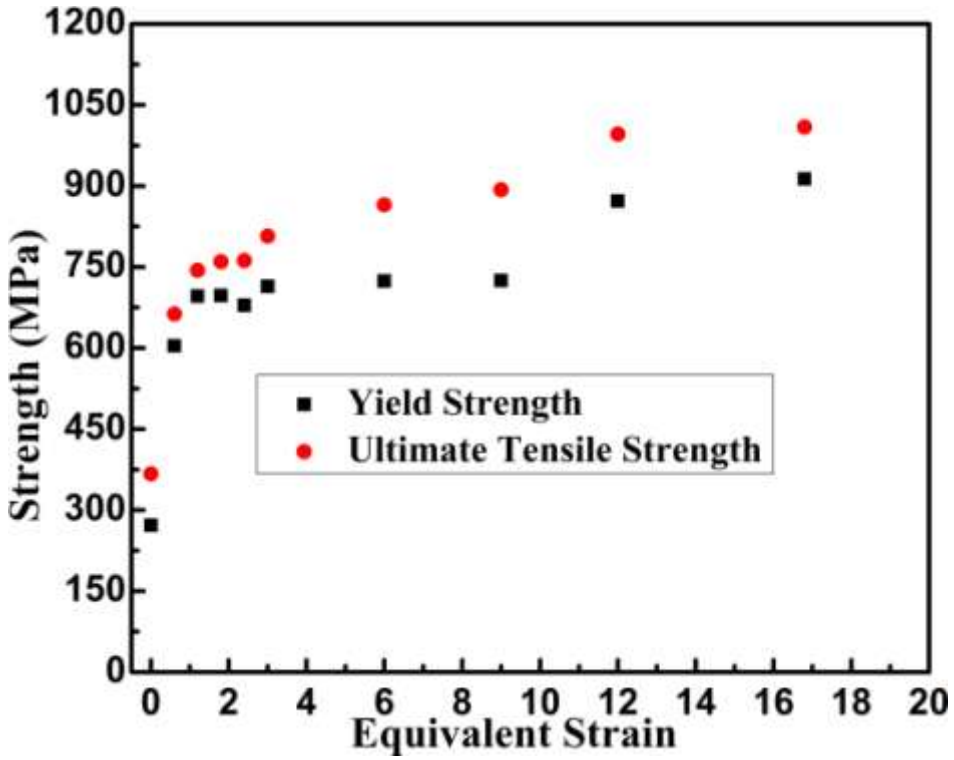

Figure 5.2 Variation in strength (YS and UTS) with equivalent strain.

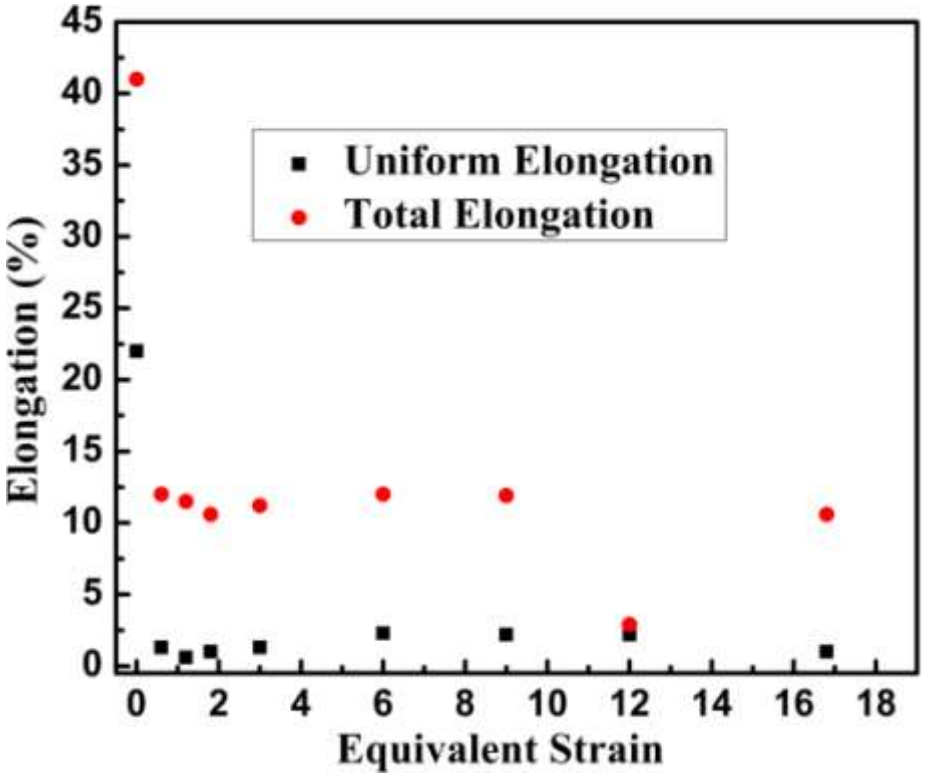

Figure 5.3 Variation in total elongation and uniform elongation with equivalent strain.

Figure 5.5 shows the plot of the microhardness vs. inverse square root of grain size for low carbon steel samples ECAPed upto ε_{vm} = 16.8. Results show that there are two linear regions on the plot from ε_{vm} = 0 – 3 and ε_{vm} = 6 - 16.8. Hall-Petch constants are calculated for each region by fitting a straight line using the method of least squares. Strain regime ε_{vm} = 0 – 3, (the fitted line A) has Hall-Patch constants $H_o^{'}$ = 1384.56 MPa and $K^{'}$ = 1.02 MPam$^{1/2}$ and for ε_{vm} = 6 – 16.8, the constant $H_o^{''}$= -5808.7 MPa and $K^{''}$ = 4.54 MPam$^{1/2}$.

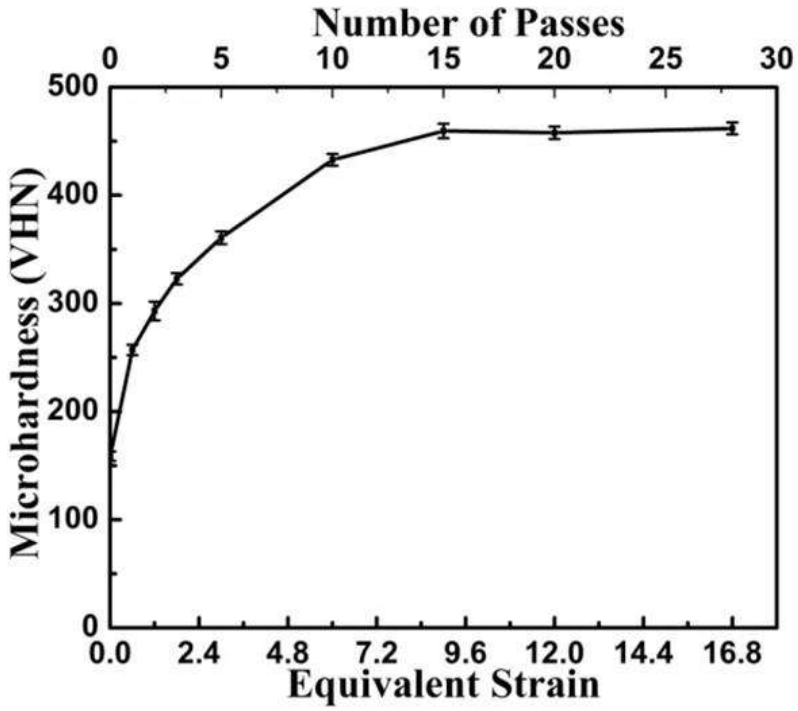

Figure 5.4 Variation in hardness with increase in equivalent strain in low carbon steel.

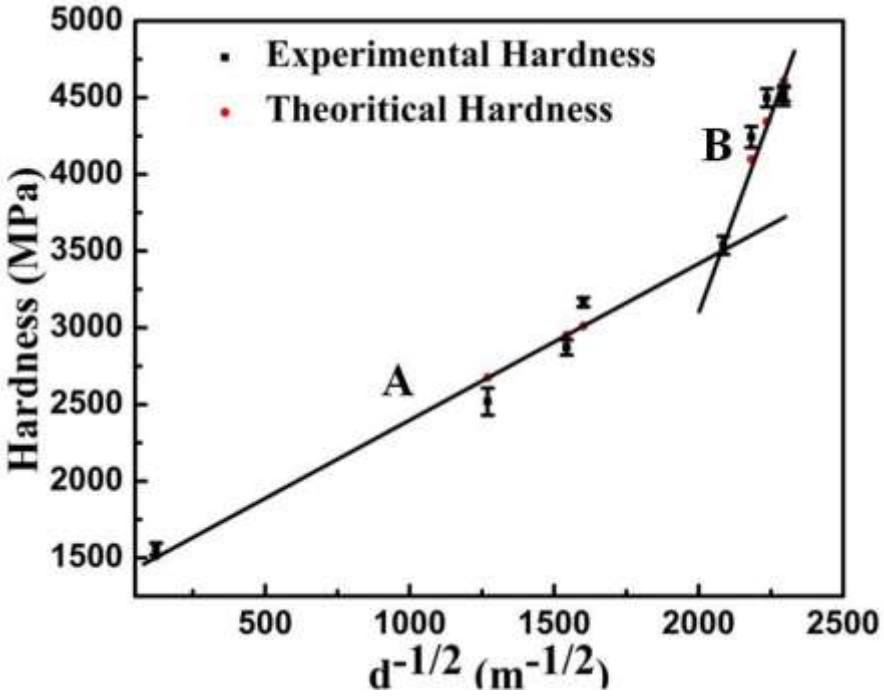

Figure 5.5 Variation of hardness and grain size ($d^{-1/2}$) for as-received and ECAPed low carbon steel.

Table 5.1: Mechanical properties of low carbon steel

Sample	(YS) (MPa)	(UTS) (MPa)	(UE) (%)	TE (%)	Hardness (VHN)	Stored Energy (J/mol)	Dimple size (μm)
As-received	272	367	22	41	159±4	44.9	37±6
ECAP-0.6	604	663	1.3	12	257±9	114	31±11
ECAP-1.2	696	744	0.6	11.5	293±5	121.5	23±6.6
ECAP-1.8	697	760	1	10.6	323±3	130.3	15±4.6
ECAP-3	714	807	1.3	11.2	361±6	125.7	12.6±5
ECAP-6	724	865	2.3	12	433±7	137.3	10±2.5
ECAP-9	725	893	2.2	11.9	460±6	129.6	4±1.5
ECAP-12	872	996	2.2	2.9	459±6	145.6	3.6±2
ECAP-16.8	913	1009	1	10.6	462±5	137.5	1.2±0.5

YS – Yield Strength, UTS – Ultimate Tensile Stength, UE – Uniform Elongation, and TE – Total Elongation.

5.2 Fractography

The fractographs of as-received low carbon steel reveal the presence of large size dimples of size 37±6 μm (Figure 5.6(a)). At ε_{vm} = 0.6, the dimple size decreases to ~8 μm (Figure 5.6(b)). From ε_{vm} = 0.6 to ε_{vm} = 6, ductile fracture (Figure 5.6(b)-(f)) is observed. The dimple size decreases with increasing strain. At ε_{vm} = 9, insignificant amount of area that too with fine dimples of 4±1.5 μm size is decreased and the sample failed by cleavage fracture. The depth of the dimples is decreased (Figure 5.6(g)) and the number of dimples per unit area is also increased. At ε_{vm} = 12, the dimple size further decreases to ~3.6±2 μm with reduced depth (Figure 5.6(h)) and increased area of cleavage fracture. A number of dimples continues to decrease with the reduced size to 1.2 μm at ε_{vm} = 16.8 (Figure 5.6(i)).

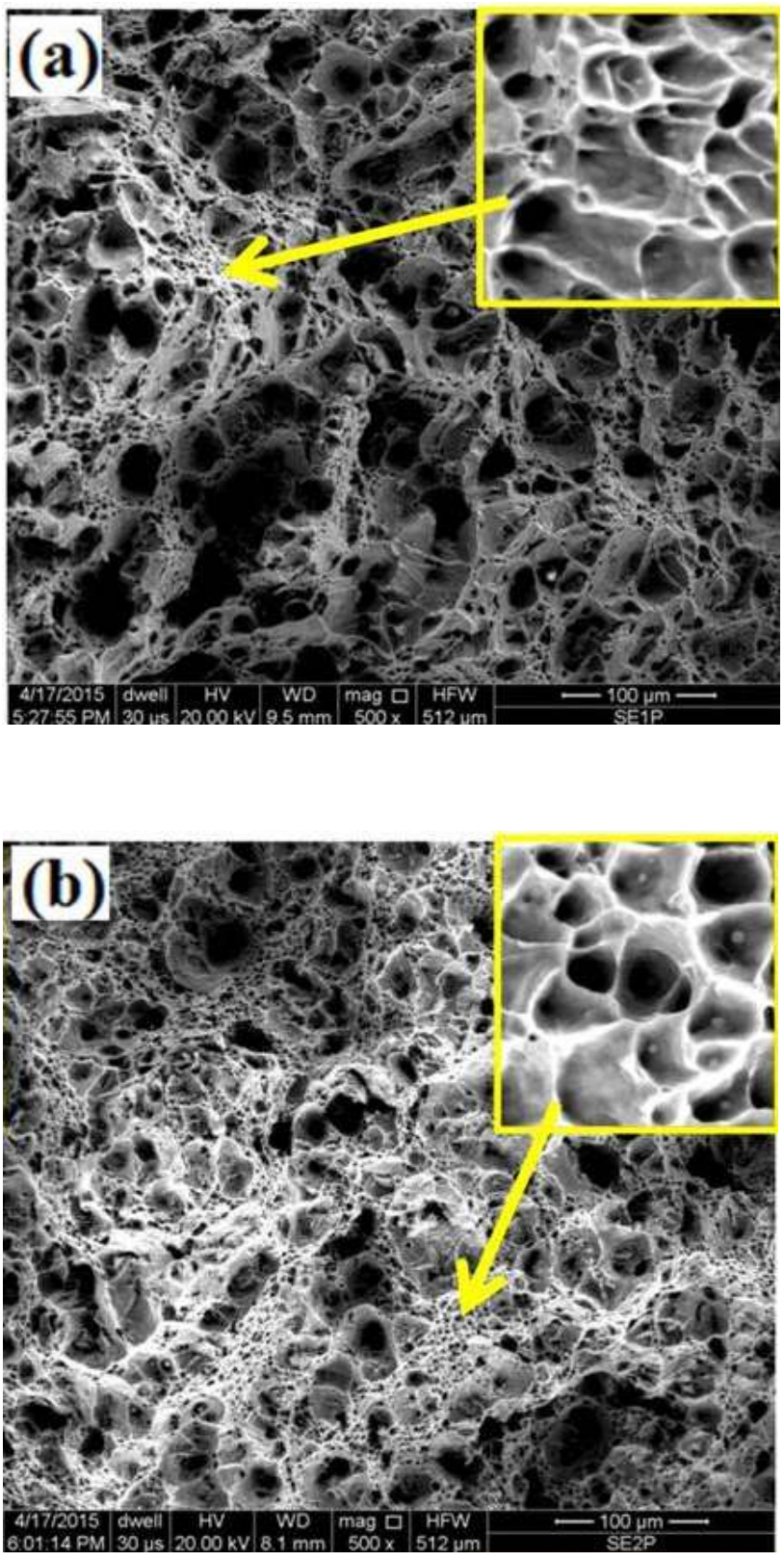

Figure 5.6 Fractographs of low carbon steel of (a) As-received, and (b) ECAP-0.6, with magnified area of fine dimples in the right hand top as indicated by arrow.

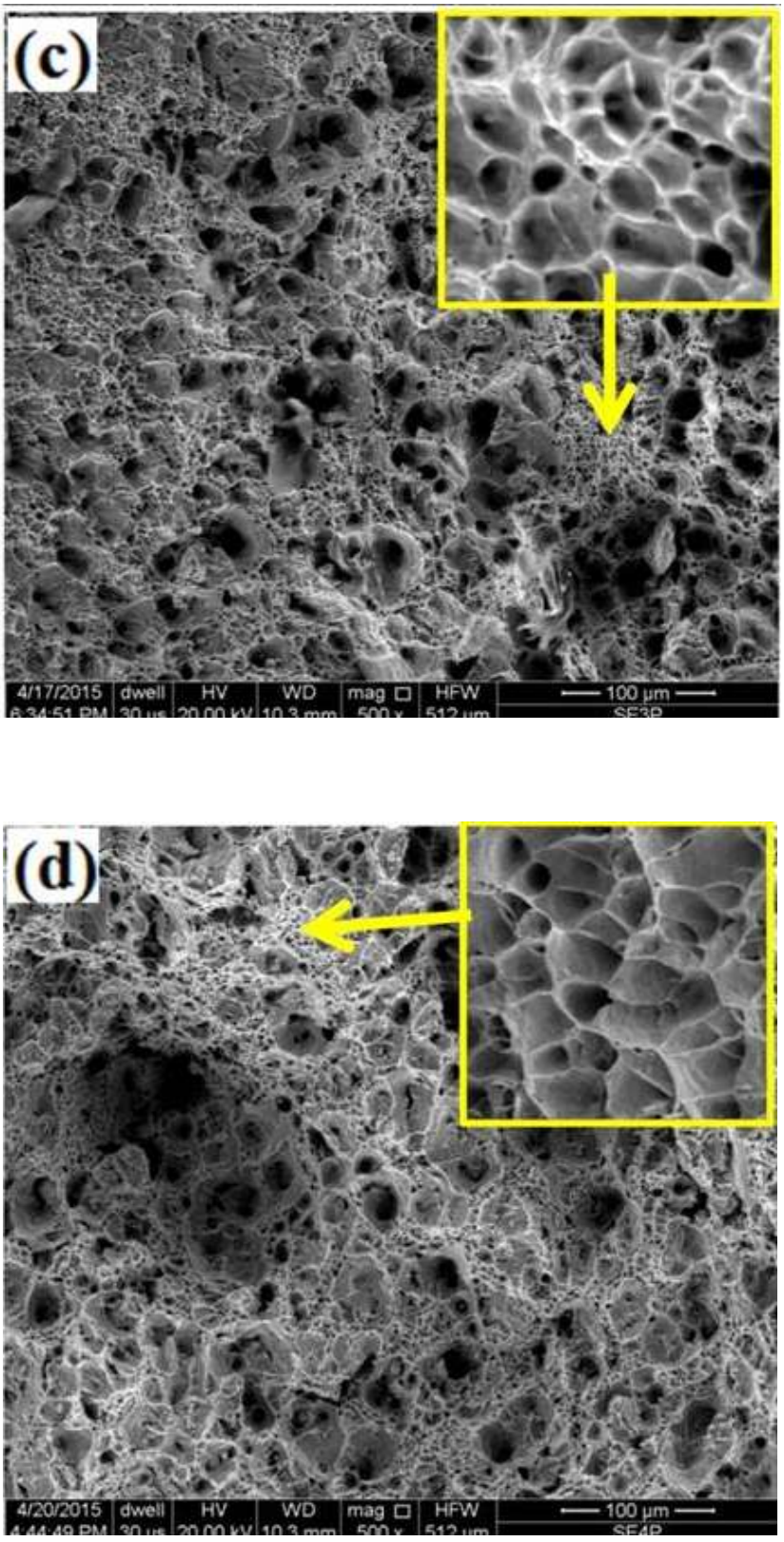

Figure 5.6 Fractographs of low carbon steel of (c) ECAP-1.2 and (d) ECAP-1.8

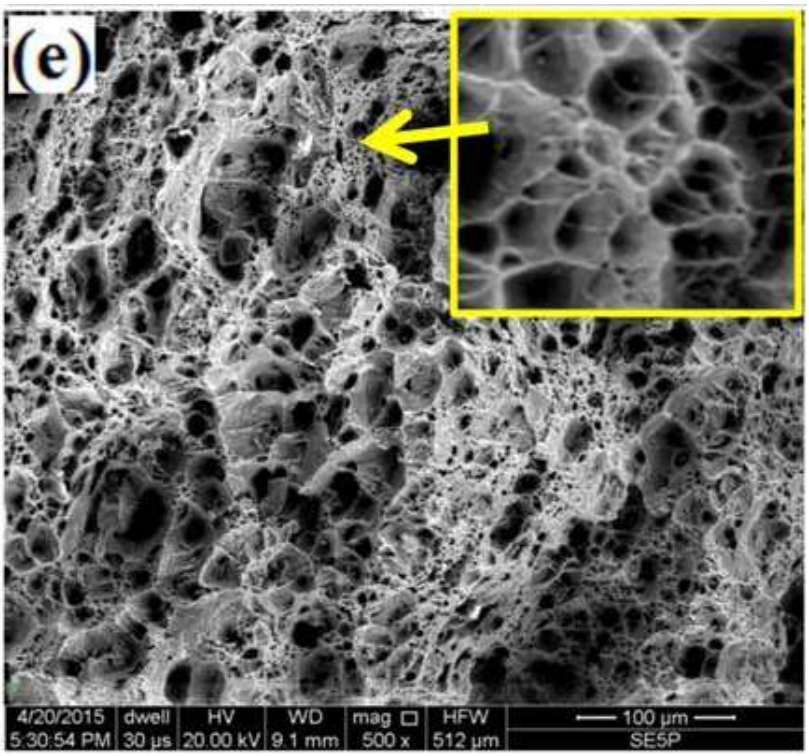

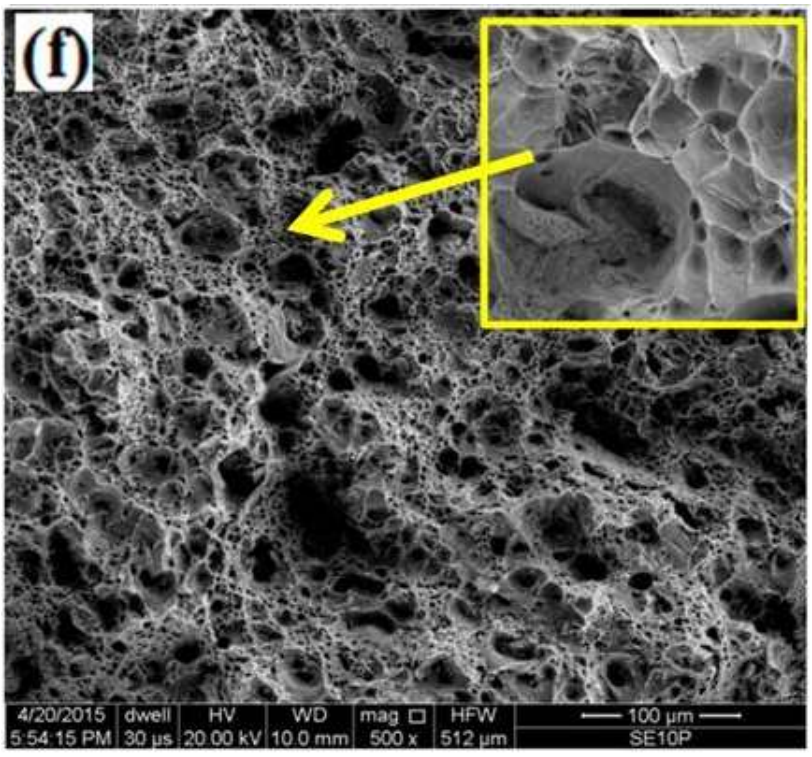

Figure 5.6 Fractographs of low carbon steel of and (e) ECAP-3, and (f) ECAP-6.

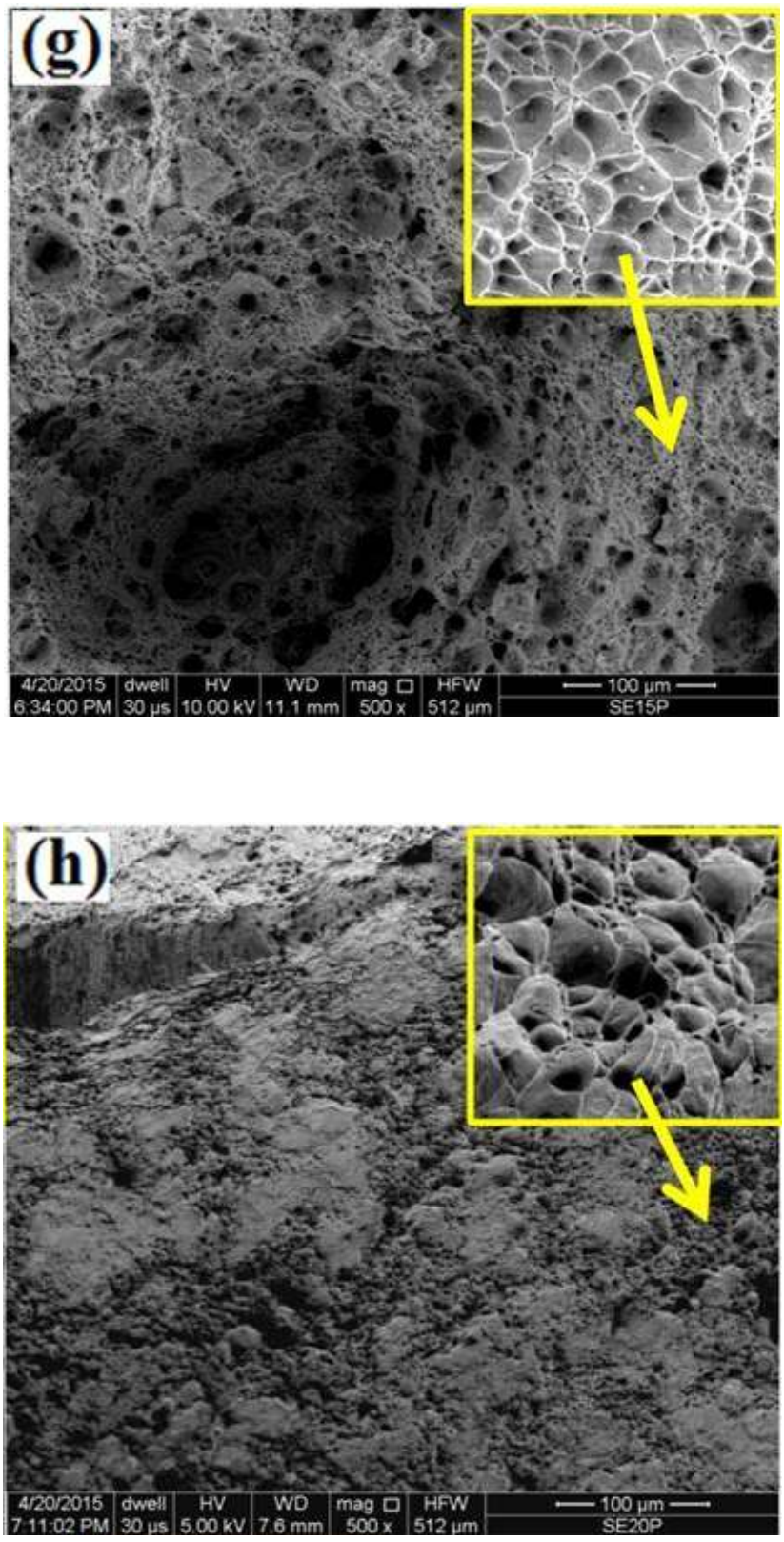

Figure 5.6 Fractographs of low carbon steel of, (g) ECAP-9, and (h) ECAP-12.

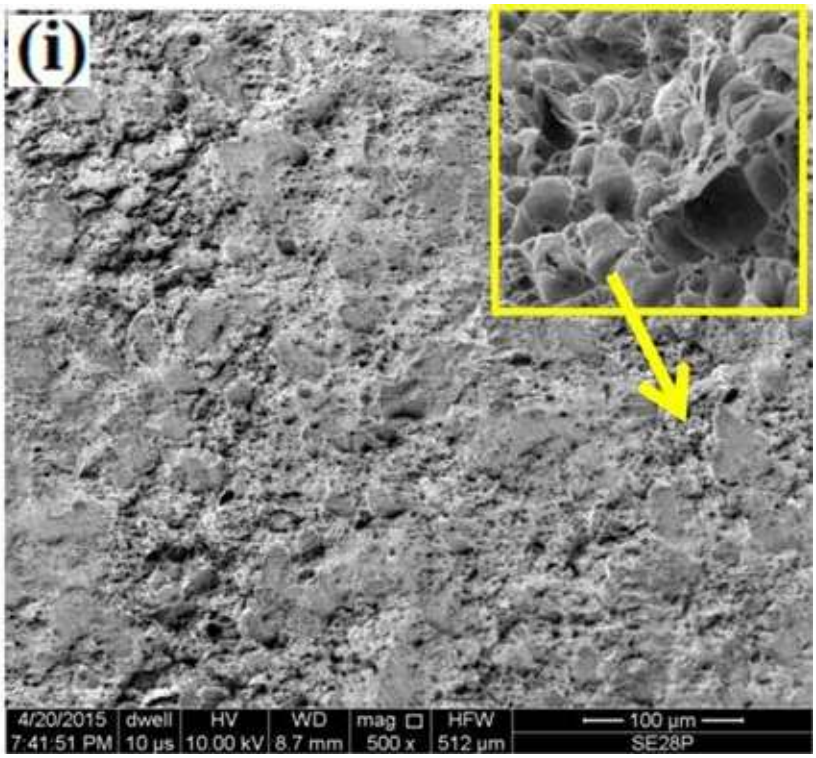

Figure 5.6 Fractographs of low carbon steel of (i) ECAP-16.8.

5.3 Discussion

The coarse-grained low carbon steel has low yield strength and ultimate tensile strength. The variation in ultimate tensile strength/yield strength with equivalent strain may be divided into five stages, ranging from stage II to VI as identified by Beygelzime et al. [Beygelzime et al. 2015]. Strengthening is steepest at the strain range ε_{vm} = 0-0.6. At ε_{vm} = 0.6, strength increases due to rapid grain refinement to the ultrafine range (0.6 µm) and a large increase in dislocation density. At ε_{vm} = 1.2, strength increases further because of the same reason. On further increase in equivalent strain (ε_{vm} = 1.8) the drastic increase in dislocation density and reduction in grain size improve strength significantly. Fukuda et al. reported similar strength for low carbon steel at low equivalent strain level (ε_{vm} = 3) [Fukuda et al. 2002]. In the strain range ε_{vm} = 0.6-1.8, the rate of strengthening decreases with

equivalent strain even though strength is higher than the previous stage. Strengthening in the range ε_{vm} = 0.6-1.8 can be denoted as stage III at which stage dislocation cell structures are formed. In intermediate strain (ε_{vm} = 3 - 6) pumping of dislocations and their annihilation by dynamic recovery occur simultaneously. Reduced grain refinement rate, annihilation of dislocations and increase in average misorientation angle of grain boundaries, enhance strength at a lower rate. Fukuda et al. and Shin et al. also observed that the strengthening at that level of strain is due to ultrafine grains and high average misorientation angle. [Fukuda et al. 2002, Shin et al. 2005]. At ε_{vm} = 6 strengthening is due to grain refinement, residual dislocation density, increase in misorientation angle, decrease in inter-lamellar spacing of pearlite and solid solution strengthening achieved by dissolution of cementite. The rate of strengthening at this stage is lower than that at low strain level due to softening by the recovery process. The strengthening by dissolution of carbides is partly compensated by the softening phenomenon.

Strengthening in the range ε_{vm} = 3-12 may be considered as stage IV at which stage strengthening continues with almost constant rate with imposed equivalent strain. At this stage fragmentation of bands, progressive build-up of new subgrain walls and shrinking of dislocation cells continue, with concurrent sharpening of cell boundaries. At higher strain level (ε_{vm} = 9 - 16.8), strength increases due to increase in average misorientation angle, significant dissolution of cementite in ferrite matrix and reduction in the size of carbides. The strengthening of the material is also attributed to grain boundary strengthening arising from thinning and decreasing of inter-lamellar spacing and solid solution strengthening from the dissolution of carbides in ferrite [Zhang et al. 2011]. At ε_{vm} = 12-16.8, strengthening rate goes down due to reduction in dislocation boundaries. This is the stage V of strengthening. Deformation of the

carbon-enriched ferrite by ECAP (ε_{vm} = 12-16.8) maintains high dislocation density which also contribute to strengthening. Therefore, at very high strain range (12-16.8), the large enhancement in strength is due to the rapid increase in misorientation angle, solid solution strengthening from the significant amount of dissolution of cementite particles, reduction in inter-lamellar spacing, rapid reduction in the size of cementite particle and high dislocation density.

The hardening behavior of the low carbon steel with equivalent strain also shows very similar trend as the strengthening. At low equivalent strain of 0-1.8, the hardness increases rapidly due to the drastic increase in the defect density and decrease in the grain size. But the rate of increase of the hardness is low at intermediate strain level (ε_{vm} = 3 - 6) due to reduced refinement rate. Therefore, the hardness remains almost constant at the higher strain level. The dislocation recovery process occurs with continuous generation and annihilation of new dislocations at higher strain level (9 - 16.8). The hardness plot with the inverse square root of grain size shows two gradients which indicate that two different mechanisms are operative for strengthening and hardening in two different strain ranges. In curve A (at low strain level upto ε_{vm} = 3) grain refinement takes place at rapid rate with increasing dislocation density. Here, strengthening is due to rapid grain refinement, and increase in dislocation density (upto ε_{vm} = 3). But at higher strain level (ε_{vm} > 6, curve B) even though refinement continues at slow rate, recovery of dislocations occur. The softening due to reduction in dislocation density is compensated by refinement in grain size, increase in average misorientation angle and dissolution of significant amount of cementite.

The as-received low carbon steel shows a large amount of uniform elongation and total elongation because grain size is in the micron range and low dislocation

density. On ECAP at low equivalent strain ductility decreases with increase in imposed strain due to the reduction in grain size in ultrafine range and drastic increase in defect density. In the intermediate strain level, ductility remains at that of low strain level due to less significant change in microstructural parameters (grain size, dislocation density, and LAGB fraction). At high strain level reduction in dislocation density, lowering of LAGB fraction and increase in misorientation angle recover uniform elongation marginally.

As-received low carbon steel has low elastic stored energy and large size dimples in the fractured surface, which are indicative of high ductility in the material. The energy required for nucleation of dimples is more than that of their growth and coalescence [Tarpani et al. 2002]. Due to lower elastic stored energy in the as-received material nucleation rate of dimples is less than that of growth rate. Here nucleation rate indicates a number of dimples per unit volume. Therefore large size dimples are observed on the fractured surface of as-received low carbon steel. At low equivalent strain, the stored energy is higher. Therefore dimple size is lower than that of the as-received material which indicates lowering of ductility. The dimple size decreases with increase in ε_{vm} due to the higher stored energy and reduced grain size [Patra et al. 2012]. At the intermediate equivalent strain range, ε_{vm} = 6 - 9, the elastic stored energy is further increased which leads to increase in nucleation of voids per unit volume and restricts the growth of voids. Therefore the significant amount of cleavage fracture is observed in the intermediate strain. Beyond a critical strain, the material fails by mixed mode of ductile and brittle fracture. The dissolution of cementite in ferrite enhances stored energy in the matrix. It increases the nucleation number and reduces sizes and depth of dimples. The minimization of the depth of the dimples is correlated to the reduction in ductility but morphological changes in

cementite from lamellar to near- spherical shape recovers ductility (≈1% in uniform elongation). At high strain level (ε_{vm} > 12) further dissolution of cementite and refinement in grain size results in significant increase in stored energy which changes the fracture behavior from ductile towards cleavage. Therefore at ε_{vm} = 16.8, the material fails mainly by cleavage or brittle fracture.

Though the mechanism of refinement in low carbon steel and IF steel are very similar, refinement process is accelerated in low carbon steel due to the presence of carbon and carbide dissolution. Dissolution of cementite in ferrite exerts solute drag force to the movement of high angle boundaries and also hinders dislocation recovery. As the selected low carbon steel was coarser than the IF steel reported by authors laboratory earlier [Verma[b] et al. 2016], at low equivalent strain grain size is higher but at intermediate strain when carbide dissolution starts, for same equivalent strain low carbon steel is finer, average misorientation angle, ultimate tensile strength, hardness and stored elastic energy of ECAPed low carbon steel are higher, dimple size and ductility are also lower than that of ECAPed IF steel. The reported IF steel is stabilized by Ti+Nb, which is almost interstitials-free. In the absence of carbon, dislocations are easily recovered, and that results in lower dislocation density which reduces the refinement rate and final grain size. Therefore, for same equivalent strain low carbon steel is finer, average misorientation angle, ultimate tensile strength, hardness and stored elastic energy of ECAPed low carbon steel are higher, dimple size and ductility are also lower than that of ECAPed IF steel.

5.4 Summary

Strength and hardness of the low carbon steel increase rapidly at early the stage of deformation at ε_{vm} = 0.6 due to the rapid rate of refining and drastic increase

in defect density, however rate of increase in strengthening decreases with increasing strain at intermediate strain range ε_{vm} = 1.2 to1.8 and formation of cellular structure, lowering of defect density. Strengthening continues in the strain range ε_{vm} = 3 to 12 with almost constant rate with respect to imposed equivalent strain due to fragmentation of bands, the formation of subgrain boundaries and shrinking of cells. Strengthening due to partial dissolution of carbides in ferrite at intermediate strain level is unable to compensate the softening effect. The mechanism of strengthening/hardening changes beyond ε_{vm} = 6 due to the significant dissolution of cementite in the ferritic matrix, in addition to lowering of defect density and increase in average misorientation angle. At the high equivalent strain ε_{vm} = 12 to 16.8, strengthening rate goes down due to a reduction in dislocation boundaries. Ultimate tensile strength of low carbon steel can be increased to >1000 MPa at ε_{vm} = 16.8 while the grain size reduces to 0.2 μm level.

On ECAP at low equivalent strain ductility decreases with increasing imposed strain due to the reduction in grain size in ultrafine range and drastic increase in defect density and stored energy. In intermediate strain, ductility remains at that low level due to less change in microstructural parameters. At high strain level (ε_{vm} = 6), reduction in dislocation density, lowering of LAGB fraction and increase in misorientation angle, recovers uniform elongation.

At the early stage of ECAP, the low carbon steel fails by ductile fracture, and with an increase in imposed strain, the size of dimples decreases as well as their number density increases with increase in stored energy. Therefore, beyond a critical equivalent strain (ε_{vm} = 9), material fails by mixed mode of ductile and brittle fracture. The amount of brittle or shear fracture increases with increasing imposed strain. As a result at ε_{vm} = 16.8, the material fails mainly by cleavage or brittle fracture.